

Special IR properties of palladium nanoparticles and their aggregations in CO molecular probe infrared spectroscopy

JIANG Yanxia, CHEN Wei, LIAO Honggang,
JIN Lanying & SUN Shigang

State Key Laboratory of Physical Chemistry of Solid Surfaces, Department of Chemistry, Xiamen University, Xiamen 361005, China
Correspondence should be addressed to Sun Shigang (e-mail: sgsun@xmu.edu.cn)

Abstract Dispersed Pd nanoparticles (Pd_n) have been synthesized by reducing H_2PdCl_4 with ethanol, and stabilized using poly(vinylpyrrolidone) (PVP). The Pd_n is applied to the glassy carbon substrate to form a thin film, and then the potential cyclic scanning at $50\text{ mV}\cdot\text{s}^{-1}$ from -0.25 to 1.25 V was carried out for about 30 min to form the aggregations of Pd_n (Pd_n^{ag}). FTIR spectroscopy of both transmission and reflection modes was employed to study CO adsorption on Pd_n and Pd_n^{ag} in both solid|liquid and solid|gas interfaces. It has been revealed that CO adsorption on Pd_n film yields two IR bands near 1964 and 1906 cm^{-1} , which are assigned to IR absorption of CO bonded on asymmetric and symmetric bridge sites, respectively. In contrast to the IR properties of CO adsorbed on Pd_n , only species of CO bonded on asymmetric bridge sites was determined on Pd_n^{ag} , and the direction of the IR band near 1963 cm^{-1} is completely inverted. The full width at half-maximum (FWHM) of the CO_B^{as} band near 1964 cm^{-1} is measured to be 14 cm^{-1} on Pd_n film, while it is 24 cm^{-1} on Pd_n^{ag} film. The results of the present study demonstrated that the inverting of the IR band direction is a general phenomenon that is closely related to the interaction between nanoparticles in aggregation of Pd_n .

Keywords: Pd nanoparticles, aggregation, CO adsorption, special IR properties, FTIRS.

DOI: 10.1360/03wb0224

Nanometer scale materials that possess the size effect, quantum effect, surface effect, and macroscopic quantum tunnel effect, etc. exhibit special properties different from bulk materials. Nowadays, the studies of nanometer scale materials have become an active foreland field of multidisciplinary, and arisen scientists' swinging interests and extensive attentions on both fundamental research and applications^[1-4]. Infrared spectroscopy is a sensitive spectroscopic method to the surface structure, by which the nature of surface and interface can be investigated at the molecule level. Hartstein et al.^[5] reported for the first time the enhancement of IR absorption (SEIRA) of organic thin films on very thin overlayer or underlayer of silver or gold in 1980. Sun and his group^[6,7] found the abnormal IR ef-

fects (AIREs) firstly in 1996 for CO adsorbed on platinum nanometer thin films prepared by electrodeposition method. In comparison with IR features of adsorbed CO, SCN^- , CN^- , etc. on bulk Pt electrodes, the same species adsorbed on corresponding nanometer scale thin film exhibit abnormal IR features, including (i) the inversion of the direction of IR bands, (ii) the enhancement of IR bands, and (iii) the widening of the full width at the half maximum (FWHM) of IR bands. Furthermore, we have found also the AIREs on the nanostructured thin films of Pt group metal or alloys (Pd, Rh, Ru, PtPd, PtRu)^[8]. Recently, Jiang et al. have prepared Pd nanoparticles in supercharges of zeolite Y by the so-called "ship-in-a-bottle" technique. The Pd nanoparticles thus formed display significant enhancement of IR absorption and the widening of FWHM for the adsorption of $CO^{[9,10]}$, but it lacks the inversion of the direction of IR band. Chen et al.^[11] have synthesized Pt nanoparticles from dispersed to agglomeration state, and studied their IR optical properties. They found that the dispersed Pt nanoparticles (Pt_n) exhibit normal enhanced IR absorption, while the agglomeration of Pt nanoparticles displays AIREs^[11]. The IR optical properties of dispersed or isolated nanoparticles are obviously different from those of the corresponding nanoscale thin film. In this paper, IR optical properties of Pd nanoparticles (Pd_n) and their aggregations (Pd_n^{ag}) are studied using transmission and reflection IR spectroscopy at both solid|liquid and solid|gas interfaces using CO as molecule probe. The goal of this study is devoted to understand the correlation between the structure and properties of low-dimension nano-materials, and further to extend the conditions producing AIREs.

1 Experimental

Pd nanoparticles (Pd_n) were synthesized by reducing H_2PdCl_4 with ethanol to metallic Pd, and stabilized with poly(vinylpyrrolidone) (PVP)^[12]. The procedure is as follows: a mixture of $15\text{ mL } 2\times 10^{-3}\text{ mol/L } H_2PdCl_4$ solution containing $4.8\times 10^{-3}\text{ mol/L HCl}$, $21\text{ mL H}_2\text{O}$, 14 mL ethanol , and 0.0667 g PVP was refluxed in a 100 mL flask for 3 h in air. The Pd_n colloid was dripped to CaF_2 window surface to form a Pd_n thin film when solvent was vaporized. The film is noted as Pd_n/CaF_2 , and is used in the course of transmission IR study. Glassy carbon (GC) was polished mechanically using alumina powders of size $0.3\text{--}5.0\text{ }\mu\text{m}$, respectively. Then GC was washed using millipore water in an ultrasonic bath for several minutes. A prescribed quantity of Pd_n colloid was applied to the surface of GC substrate, upon which a drop solution of dichloroethane containing polyvinyl chloride (PVC) was dispersed to fix Pd_n on GC surface. A thin film electrode was thus formed on the GC substrate after solvent evaporation, and was noted as Pd_n/GC . A CHI-660A potenti-

ARTICLES

stat/galvanostat (Shanghai Chenhua Instruments, Inc.) was used in electrochemical studies. A three-electrode cell was employed. Pd_n/GC is used as working electrode, a foil of platinum black as count electrode, and the saturated calomel electrode (SCE) as the reference electrode. The potentials reported in the present paper are referred to the SCE scale. All experiments were carried out at room temperature around 20°C. Pd_n^{ag}/GC was prepared by applying a potential cyclic scanning from -0.25 to 1.25 V for about 30 min with a scan rate of 50 mV·s⁻¹. Transmission Electron Microscopy (TEM) (JEM-100CX-II) and Scanning Electron Microscopy (SEM) (LEO 1530) were used to inspect the morphology and measure the mean size of Pd nanoparticles. Transmission and reflection FTIR spectroscopic experiments at both solid|liquid and solid|gas interfaces, and electrochemical *in situ* FTIR reflection experiment at solid|liquid interface were carried out on a Nexus 870 FTIR spectrometer (Nicolet) equipped with an EverGlo™ IR source and a liquid nitrogen-cooled MCT-A detector.

2 Results and discussion

(i) TEM and SEM studies. The TEM image of Pd_n is shown in Fig. 1(a). The well-dispersed Pd_n pellets are observed, and the interaction between the Pd_n pellets may be omitted. The average size is measured about 3 nm. The SEM image of Pd_n^{ag} is shown in Fig. 1(b). It can be observed that Pd_n^{ag} particles are distributed in different domains, and they are closely packed in each domain. The average size of Pd_n^{ag} was measured about 17 nm.

(ii) Cyclic voltammetric studies. The solid line in Fig. 2 shows cyclic voltammogram (CV) of Pd_n/GC recorded between -0.25 and 1.25 V for the first potential cyclic scanning in 0.1 mol·L⁻¹ H₂SO₄ solution with a scan rate of 50 mV·s⁻¹. Two distinct current peaks around -0.14 and -0.06 V are the characteristic potentials for hydrogen adsorption-desorption. A positive-going oxidation peak at 0.62 V is observed, and the following Pd ox-

ide is formed above 0.8 V in the positive-going potential scanning. In the reverse scan, a small current peak of reduction of Pd oxide is appeared at 0.40 V. We found that the oxidation peak at 0.62 V decreased, accompanying an increase of current of adsorption-desorption of hydrogen and oxygen when the number of potential cyclic scanning augmented. After the potential cyclic scanning was lasted for 30 min, the oxidation peak at 0.62 V disappeared, and the Pd nanoparticles have been aggregated, noted as Pd_n^{ag}/GC. The stable CV is shown as the dashed line in Fig. 2. We can observe a pair of hydrogen adsorption and desorption at -0.14 and -0.06 V, and an oxidation current above 0.48 V attributed to the formation of Pd oxide species on Pd_n^{ag}/GC, and the reduction current peak of Pd oxide at 0.32 V. In comparison with the CV of Pd_n/GC, the oxidation current peak at 0.62 V disappeared, which was accompanied by the increasing of current peak amplitude of adsorption-desorption of hydrogen and oxygen. The above CV results demonstrate that the species of irreversible adsorption occupied initially the active sites on Pd_n/GC, which suppressed the adsorption-desorption of hydrogen and oxygen. When the species have been removed by oxidation, the adsorption-desorption current peak amplitude increases. The Pd nanoparticles in electrode were changed from the dispersed state to aggregative state in above process. The protecting mechanism of PVP used to stabilize and disperse Pd_n may suggest that the carbonyl groups of PVP are partly coordinated to Pd atoms of the Pd nanoparticles^[13-15]. Therefore, we infer that the species with irreversible adsorption is carbonyl groups in PVP. In the course of potential cyclic scanning from -0.25 to 1.25 V, the stabilizer PVP is oxidized and dissolved gradually into solution. Under the perturbation of interfacial electric field the dispersed Pd nanoparticles may be migrated in the film and aggregated to form Pd_n^{ag}, as a consequence the interaction between Pd nanoparticles is increased. In our FTIR investigations we have observed carbonyl groups IR band at 1683 cm⁻¹ on Pd_n/GC, while

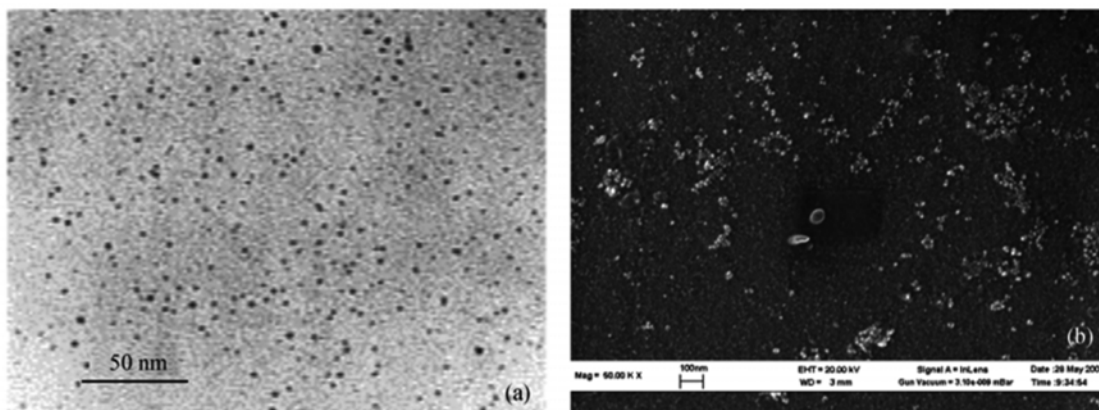


Fig. 1. (a) TEM image of Pd_n, (b) SEM image of Pd_n^{ag}/GC.

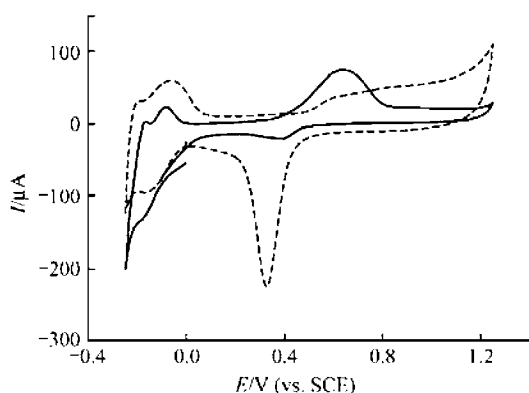


Fig. 2. Comparison of cyclic voltammograms recorded on Pd_n/GC (solid line) and Pd_n^{ag}/GC (broken line); 0.1 mol·L⁻¹ H₂SO₄ solution, 50 mV·s⁻¹.

the same IR band cannot be observed when Pd_n^{ag}/GC is formed.

The potential cyclic scanning was carried out from -0.25 to 0.10 V, in which CO was bubbled into solution for 30 min to reach a saturation adsorption of CO on the surface of Pd_n^{ag}/GC, and then N₂ was bubbled into solution for 10 min to remove CO in solution. The CV curve of the oxidation of adsorbed CO (CO_{ad}) on Pd_n^{ag}/GC is displayed in Fig. 3. It can be seen that the hydrogen adsorption-desorption current is suppressed when electrode surface is covered with CO. In the positive-going potential scanning, CO_{ad} is oxidized, and gives rise a current peak centered at 0.72 V. Hydrogen adsorption-desorption current peak can be seen again after CO_{ad} oxidation. It is worth noting that the potential of the oxidation peak of CO on Pd_n^{ag}/GC is higher than that on bulk Pd under the same conditions. It can be reasonably interpreted that the surface active sites on Pd_n^{ag}/GC were held partly by carbonyl groups on PVP. This leads to the inhibition of adsorption of the active oxide species. As the oxidation of CO_{ad} involves active oxygen species on Pd_n^{ag}/GC surface,

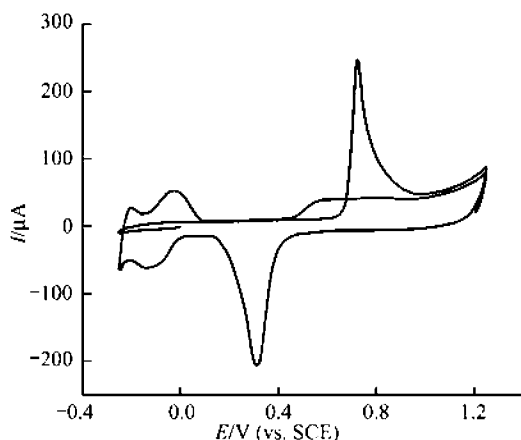


Fig. 3. Cyclic voltammograms of CO_{ad} oxidation on Pd_n^{ag}/GC. 0.1 mol·L⁻¹ H₂SO₄ solution, 50 mV·s⁻¹.

the potential of CO_{ad} oxidation on Pd_n^{ag}/GC is consequently increased. We have tested that, moreover, Pt_n (2.5 nm) cannot form aggregation under the same electrochemical condition, demonstrating that the aggregative phenomenon is related to metal itself properties.

(iii) IR optical properties of Pd_n and Pd_n^{ag}

(1) Transmission and reflection FTIR spectroscopy at solid|gas interfaces. In the *in situ* transmission or reflection FTIR experiments at solid|gas interfaces, Pd_n/CaF₂, Pd_n/GC, or Pd_n^{ag}/GC were respectively assembled to corresponding homemade IR cell. The single-beam spectrum of background (R_B) was collected at first during bubbling N₂, and then the single-beam spectrum of sample (R_S) was recorded after bubbling CO gas to cell for 5 min. The resulting spectrum was reported as conventional absorption spectrum, which is calculated as

$$A = -\log(R_S/R_B), \quad (1)$$

500 interferograms of spectral resolution 2 cm⁻¹ were scanned into R_S and R_B , respectively. The transmission resulting spectrum of Pd_n/CaF₂, and the reflection resulting spectra of Pd_n/GC and Pd_n^{ag}/GC are shown in Fig. 4. The transmission resulting spectrum of CO adsorbed on Pd_n/CaF₂ exhibits four bands (Fig. 4(a)). A pair of positive-going bands centered at 2143 cm⁻¹ with P and R lines was assigned to the IR absorption of gaseous CO species (CO_g). The other two positive-going IR bands centered at 1964 and 1905 cm⁻¹ attributed to the IR absorption of CO bonded to asymmetric and symmetric bridge sites (CO_B^{as} and CO_B^s) at the edges and facets of Pd_n^[16,17], respectively. The full width at half maximum (FWHM) of both CO_B^{as} and CO_B^s is determined to be 14 cm⁻¹ on Pd_n/CaF₂. The intensity of IR band of CO_B^s at 1905 cm⁻¹ is much stronger than that of CO_B^{as} at 1964 cm⁻¹. The IR bands of CO_B^{as} and CO_B^s are appeared in the same direction of the CO_g bands, indicating that Pd_n gives rise to normal IR absorption. The reflection resulting spectrum of Pd_n/GC was obtained as it was done in transmission pattern. The reflection resulting spectrum of CO adsorbed on Pd_n/GC (Fig. 4(b)) is identical to that in Fig. 4(a). The results in Fig. 4 (a) and (b) demonstrate that the electrode substrates, the incidence angle of IR, and the polarized light do not affect the shape and the intensity of resulting spectrum. Fig. 4(c) gives a reflection resulting spectrum of CO adsorbed on Pd_n^{ag}/GC. The IR features differ from those of CO adsorbed on Pd_n/GC in the following respects: first, the direction of the CO_B band is inverted from positive-going to negative-going; second, the FWHM of the CO_B band increases to 24 cm⁻¹ that is larger than the value of 14 cm⁻¹ on Pd_n/GC; third, the peak at 1905 cm⁻¹ for CO bonded to symmetric bridge sites disappears. It is evident that Pd_n^{ag}/GC produces abnormal IR band for the adsorption of CO. The sizes of Pd_n^{ag} are non-uniform, and the numbers of different surface sites on Pd_n^{ag} are more than that on Pd_n, which may generate inhomogeneous broadening of CO

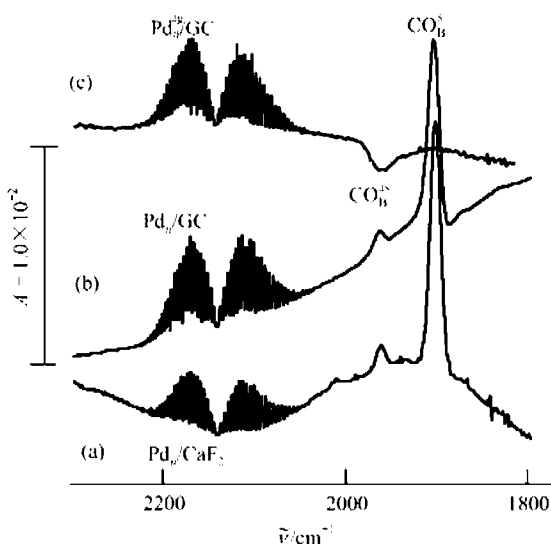


Fig. 4. FTIR spectra of CO_{ad} on Pd_n/CaF_2 , Pd_n/GC and $\text{Pd}_n^{\text{ag}}/\text{GC}$, at solidgas interface.

band^[17]. The above results from transmission and reflection at solid|gas interfaces illustrated that the IR optical properties of Pd nanoparticles depend mainly on the aggregation state of nanoparticles, and scarcely on the transmission or reflection mode of FTIR spectroscopy.

(2) *In situ* FTIR reflection spectroscopy at solid|liquid interfaces. CO adsorption on $\text{Pd}_n^{\text{ag}}/\text{GC}$ was carried out by introducing pure CO gas into $0.1 \text{ mol} \cdot \text{L}^{-1} \text{H}_2\text{SO}_4$ solution, accompanying potential cyclic scanning between -0.25 and 0.20 V for 30 min to ensure a saturation adsorption of CO. CO species in solution were then removed completely by bubbling pure N_2 gas into the solution for 10 min along with continuous potential cyclic scanning between -0.25 and 0.20 V to prevent CO_{ad} oxidation. The single beam spectra $R(E_S)$ were collected at different E_S varying from -0.25 to 0.20 V at first. It is known that the

CO_{ad} species are stable at these potentials of E_S . The E_R was set at 1.25 V , where CO_{ad} was oxidized immediately into CO_2 species. The single beam spectrum $R(E_R)$ was thus recorded at E_R . The resulting spectra are the potential difference spectra, which is expressed as follows:

$$\Delta R/R = (R(E_S) - R(E_R))/R(E_R) \quad (2)$$

According to the above description, only CO_{ad} exists at E_S , and they are oxidized completely into CO_2 entering into the solution of thin layer between electrode and IR window. Fig. 5 shows a series of MSFTIR spectra of CO adsorbed on $\text{Pd}_n^{\text{ag}}/\text{GC}$ at $0.1 \text{ mol} \cdot \text{L}^{-1} \text{H}_2\text{SO}_4$ solution at different E_S . The positive-going band near 1963 cm^{-1} is observed in all spectra, which is attributed to IR absorption of CO_B^{as} at E_S . The FWHM of the CO_B^{as} band is measured to be 24 cm^{-1} , which is larger than the value of 14 cm^{-1} measured in the spectrum of Pd_n . A positive-going IR band at 2345 cm^{-1} can be also observed, which is ascribed to the IR absorption of CO_2 species at E_R . In general, the IR bands direction of CO_B is negative-going, and that of CO_2 is positive-going as predicted by Eq. (2). From Fig. 5(a) we see that CO_B^{as} bands appear in the same direction as that of CO_2 band does, illustrating that the absorption of CO_B^{as} on $\text{Pd}_n^{\text{ag}}/\text{GC}$ produces abnormal IR band. In comparison with CO adsorbed on bulk Pd^[9], the enhanced factor is accounted for 4.8 for CO adsorbed on $\text{Pd}_n^{\text{ag}}/\text{GC}$. Fig. 5(b) shows the potential dependence of IR band center of CO_B^{as} on $\text{Pd}_n^{\text{ag}}/\text{GC}$, in which the center of the CO_B^{as} band is blue-shifted following the increase of E_S . The stark effect that represents the affection of electric field on the adsorbed molecule, i.e. $d\tilde{\nu}_{\text{CO}_B^{\text{as}}}/dE_S$, can be determined from the slope of the linear relationship between $\tilde{\nu}_{\text{CO}_B^{\text{as}}}$ and E_S . A value of $27 \text{ cm}^{-1} \cdot \text{V}^{-1}$ is determined from Fig. 5(b), which is smaller than that of $47 \text{ cm}^{-1} \cdot \text{V}^{-1}$ on bulk Pd^[18].

It is known that the special IR optical properties are

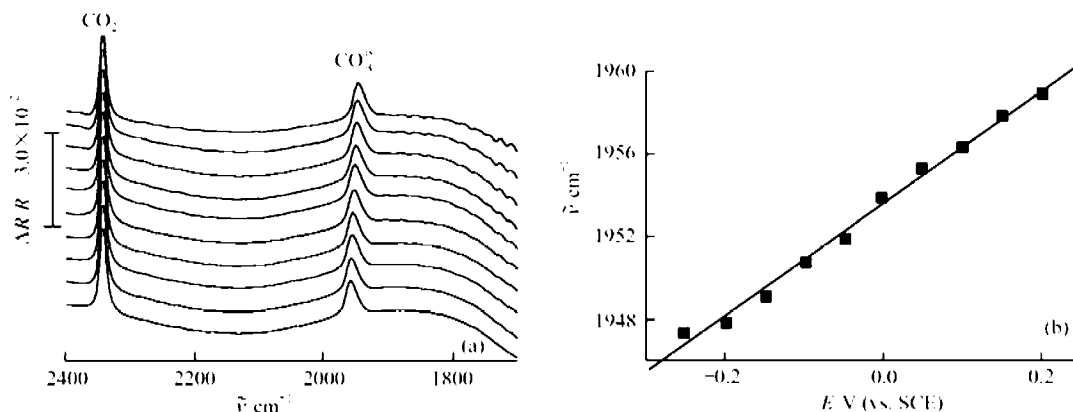


Fig. 5. (a) MSFTIR spectra of CO adsorbed on $\text{Pd}_n^{\text{ag}}/\text{GC}$ $0.1 \text{ mol} \cdot \text{L}^{-1} \text{H}_2\text{SO}_4$ solution, $E_R = 1.25 \text{ V}$, E_S is changed from -0.25 to 0.2 V (from top to bottom) by the step of 50 mV ; (b) potential dependence of IR band center of CO_B on $\text{Pd}_n^{\text{ag}}/\text{GC}$.

correlated with the surface structure of nanometer scale materials. Based on the literature, the materials produced AIREs, for example, both the nanometer thin film^[8] and Pt_n agglomeration with nafion as stabilizer^[11], the particles are overlapped during the electrodeposition in the former system, and the particles edges are close contacted each other with the help of nafion film in the latter system. In the current paper, the results demonstrated that the interaction between nanoparticles leads to appear the AIREs.

3 Conclusions

In this paper, dispersed Pd nanoparticles (Pd_n) of ca. 3 nm in diameter were synthesized by reducing H₂PdCl₄ with ethanol. The PVP was used as the stabilizer. The interaction between the particles can be omitted between Pd_n. The aggregative state Pd_n^{ag} with the size of 17 nm was formed by cyclic potential scanning from -0.25 to 1.25. A strong interaction between Pd_n in the Pd_n^{ag} is suggested to appear. The IR spectroscopic studies of both solid|gas and solid|liquid interfaces have illustrated that CO adsorbed on dispersed Pd_n gives rise to enhanced IR absorption (EIRA), while on the aggregative Pd_n^{ag} produces abnormal effects (AIREs). The results illustrated that the interaction between nanoparticles makes the inverting of the IR band direction of adsorbed CO species. The present studies are of significant importance for understanding the special optical properties of nanometer materials.

Acknowledgements This work was supported by the National Natural Science Foundation of China (Grant Nos. 20173045, 90206039, and 20021002), the National Key Basic Research and Development Program (Grant No. 2002CB211804).

References

1. Fei, L., Analysis of Nanomaterials (in Chinese), Beijing: Chemistry Industry Press, 2003, 1—356.
2. Lue, J. -T., A review of characterization and physical property studies of metallic nanoparticles, *J. Phys. Chem. Solids*, 2001, 62: 1599—1612.
3. Haruta, M., Date, M., Advances in the catalysis of Au nanoparticles, *Appl. Catal. A-Gen.*, 2001, 222: 427—437.
4. Brust, M., Kiely, C. J., Some recent advances in nanostructure preparation from gold and silver particles: a short topical review, *Colloid Surface A*, 2002, 202: 175—186.
5. Hartstein, A., Kirtly, J. R., Tsang, T. C., Enhancement of the infrared-absorption from molecular monolayers with thin metal overlayers, *Phys. Rev. Lett.*, 1980, 45(3): 201—204.
6. Lu, G. Q., Sun, S. G., Chen, S. P. et al., Abnormal Optic properties of dispersed platinum layer in FTIR reflection spectroscopy for CO adsorption, in *Electrode Processes, PV96-8* (eds. Wieckowski, A., Itaya, K.), New Jersey: The Electrochemical Society, Inc., 1996, 436—445.
7. Lu, G. Q., Sun, S. G., Cai, L. R. et al., *In situ* FTIR spectroscopic studies of adsorption of CO, SCN⁻, and poly (*o*-phenylenediamine) on electrodes of nanometer thin films of Pt, Pd, and Rh: The abnormal infrared effects (AIREs), *Langmuir*, 2000, 16: 778—786.
8. Sun, S. G., Abnormal infrared effects of nanometer-scale thin film material of platinum group metals and alloys at electrode-electrolyte interfaces, in *Catalysis and Electrocatalysis at Nanoparticle Surfaces* (eds. Wieckowski, A., Savinova, E. R., Vayenas, C. G.), New York: Marcel Dekker Inc., 2003, 785—826.
9. Jiang, Y. X., Sun, S. G., Chen, S. P. et al., Novel phenomenon of enhancement of IR absorption of CO adsorbed on nanoparticles of Pd confined in supercages of Y-zeolite, *Chem. Phys. Lett.*, 2001, 344: 463—470.
10. Jiang, Y. X., Sun, S. G., Chen, S. P. et al., Enhancement of IR absorption of CO adsorbed on palladium-loading zeolite thin film electrode, *Chem. J. Chinese University* (in Chinese), 2001, 11: 1860—1863.
11. Chen, W., Sun, S. G., Zhou, Z. Y., et al., IR optical properties of Pt nanoparticles and their agglomerates investigated by *in situ* FTIRS using CO as probe molecule, *J. Phys. Chem. B*, 2003, 107: 9808—9812.
12. Li, Y., Boone, E., El-Sayed, M. A., Size effects of PVP-Pd nanoparticles on the catalytic Suzuki reactions in aqueous solution, *Langmuir*, 2002, 18: 4921—4925.
13. Teranishi, T., Hosoe, M., Tanaka, T. et al., Size control of mono-dispersed Pt nanoparticles and their 2D organization by electro-phoretic deposition, *J. Phys. Chem. B*, 1999, 103: 3818—3827.
14. Teranishi, T., Miyake, M., Size control of palladium nanoparticles and their crystal structures, *Chem. Mater.*, 1998, 10: 594—600.
15. Reetz, M. T., Winter, M., Tesche, B., Self-assembly of tetraalkylammonium salt stabilized giant palladium clusters on surfaces, *Chem. Commun.*, 1997: 147—148.
16. Wolter, K., Seiferth, O., Kuhlenbeck, H. et al., Infrared spectroscopic investigation of CO adsorbed on Pd aggregated deposited on an alumina model support, *Surface Science*, 1998, 399: 190—198.
17. Hoffmann, F. M., Infrared reflection-absorption spectroscopy of adsorbed molecules, *Surf. Sci. Rep.*, 1983, 3: 107—192.
18. Ding, N., Jiang, Y. X., Sun, S. G., Novel IR properties of Pd nanoparticles confined in supercages of Y-zeolite in CO adsorption at electrochemical solid/liquid interfaces, in *Quantum Confinement VI: Nanostructured Materials and Devices* (eds. Cahay, M., Leburton, J. P., Lockwood, D. J. et al.), New Jersey: The Electrochemical Society, Inc., 2001, 34—52.

(Received December 15, 2003; accepted May 14, 2004)